Journal of Nematology 34(3):213–221. 2002.

Discriminating *Tsuga canadensis* Hemlock Forest Defoliation Using Remotely Sensed Change Detection[1]

D. D. Royle[2] and R. G. Lathrop[3]

Abstract: The eastern hemlock (*Tsuga canadensis*) is declining in health and vigor in eastern North America due to infestation by an introduced insect, the hemlock woolly adelgid (*Adelges tsugae*). Adelgid feeding activity results in the defoliation of hemlock forest canopy over several years. We investigated the application of Landsat satellite imagery and change-detection techniques to monitor the health of hemlock forest stands in northern New Jersey. We described methods used to correct effects due to atmospheric conditions and monitor the health status of hemlock stands over time. As hemlocks defoliate, changes occur in the spectral reflectance of the canopy in near infrared and red wavelengths—changes captured in the Normalized Difference Vegetation Index. By relating the difference in this index over time to hemlock defoliation on the ground, four classes of hemlock forest health were predicted across spatially heterogeneous landscapes with 82% accuracy. Using a time series of images, we are investigating temporal and spatial patterns in hemlock defoliation across the study area over the past decade. Based on the success of this methodology, we are now expanding our study to monitor hemlock health across the entire Mid-Atlantic region.

Key words: Adelges tsugae, change detection, defoliation, discriminant analysis, discriminating, eastern hemlock, forest, hemlock woolly adelgid, Landsat TM, remote sensing, *Tsuga canadensis.*

The eastern hemlock (*Tsuga canadensis* Carriere) is an important native conifer in the forests of the northeastern United States and southern Canada, where it is highly valued for its ecological, cultural, and economic significance (Quimby, 1996). One of the major forest health issues impacting the eastern United States is the declining health and dieback of the eastern hemlock by the hemlock woolly adelgid (HWA) (*Adelges tsugae* Annand), an introduced Asian insect (Lashomb et al., 2002; McClure, 1987; McManus et al., 1999; Salom et al., 1996). Dispersed by wind, birds, and mammals (McClure, 1990), this tiny (1-mm), sap-feeding, aphid-like insect has spread into at least 15 eastern states since its introduction around 1950 (Onken, 2002; Stoetzel, 2002). As a result of this infestation, hemlock is threatened throughout its natural range (Souto et al., 1996). Hemlock defoliation and mortality have been high over the past decade in the Mid-Atlantic region, especially in northern New Jersey (Royle and Lathrop, 1997) and neighboring eastern Pennsylvania, where hemlock is an important natural feature in numerous local, state, and national parks and forests (Evans et al., 1996).

Modeling hemlock vulnerability to HWA, based on site and landscape characteristics, is an important goal in hemlock research (Williams et al., 2002). Information about the location of hemlock stands, their current condition, and the rate at which they are declining is crucial for analyses that examine the effects of hemlock defoliation and mortality on ecological processes and forest succession (Lashomb et al., 2002; McManus et al., 1999). In addition, this information would be useful for selecting stands in which to release natural predators of HWA (Cheah and McClure, 2002). The first step in modeling hemlock vulnerability, however, is to map and quantify hemlock forest health at the appropriate temporal and spatial scales with the highest possible accuracy.

Remote sensing provides an efficient, cost-effective means for monitoring forest health (Lachowski et al., 1992). It has been used to detect, quantify, and map forest canopy defoliation by a number of insect herbivores including spruce budworm (Franklin and Raske, 1994) and gypsy moth (Muchoney and Haack, 1994). In the mid-1990s, we undertook a pilot study to investigate the utility of satellite imagery and image-processing techniques to monitor eastern hemlock forest health. To minimize differences in solar illumination and vegetation phenology between scenes, we used anniversary dates (1984 and 1994) of Landsat Thematic Mapper (TM) imagery (i.e., Landsat images acquired at about the same time of year). We detected and quantified our levels of canopy defoliation of eastern hemlock forest by HWA for a 1,625-km^2 study area in northern New Jersey with a classification accuracy of 64% for four levels of defoliation, and 70% to 72% accuracy for three levels of defoliation (Royle and Lathrop, 1997). Since that time, we have investigated further refinements to our initial study with the objective of developing a robust methodology suitable for monitoring hemlock forest health across a heterogeneous landscape at the regional scale, i.e., thousands of square kilometers.

Challenges in remotely sensed detection of HWA defoliation: The application of remote sensing technology to forest health monitoring is beset by a number of challenges. As in any change-detection project, positional inaccuracy, atmospheric haze, and terrain shadowing are complicating factors that must be addressed. Additionally, the spatial heterogeneity of naturally occurring hem-

Received for publication 11 September 2001.

Paper delivered in a symposium on Application of GIS and GPS Precision Agriculture Technologies in Nematology and Plant Pathology, Society of Nematologists Annual Meeting 24–29 August 2001, Salt Lake City, UT.

[1] Supported in part by grants from the U.S. Department of Agriculture Forest Service and the New Jersey Agricultural Experiment Station.

[2] Graduate Assistant, Center for Remote Sensing and Spatial Analysis, Rutgers University, New Brunswick, NJ 08901.

[3] Director, Center for Remote Sensing and Spatial Analysis, Rutgers University, New Brunswick, NJ 08901.

The authors thank Colleen Hatfield, Faiz Rahman, and anonymous reviewers for helpful comments, and the USDA Forest Service and NJ Forestry for their ongoing support.

E-mail: lathrop@crssa.rutgers.edu

This paper was edited by B. C. Hyman.

lock stand structure in a complex landscape presents special challenges not normally encountered in an agricultural setting.

The nature and course of HWA defoliation determines the appropriateness of various techniques designed to detect changes in forest canopies. Hemlock woolly adelgid defoliation is characterized as a slow loss of needles and a reduction in new growth, generally progressing from the lower branches upward to the top of the crown. Thus, HWA damage appears as a general thinning of foliage taking place over the course of several years, though tree death can occur in 2 to 4 years (McClure, 1987). Hemlock woolly adelgid damage symptoms differ from those of some other forest insects (e.g., spruce budworm) in that there are no distinct changes in the color of damaged foliage, although hemlock needles can take on a grayish cast as they desiccate from loss of fluids.

Various methods have been used to detect and quantify defoliation in forest canopies (Bannari et al., 1995; Coppin and Bauer, 1996; Singh, 1989). One method, image classification (Jensen, 1986), identifies spectral clusters that represent different levels of defoliation among forest stands, usually within a single date of imagery. In most cases, image classification exploits changes in the color of tree foliage attacked by insects. This method was used to monitor defoliation by spruce budworm (Buchheim et al., 1985; Leckie and Ostaff, 1988), hemlock looper (Franklin, 1989), and gypsy moth (Muchoney and Haack, 1994). Detecting subtle changes in color in hemlock foliage infested by HWA, however, is difficult in mixed forests with varying amounts of hemlock, especially in rugged terrain. Another method, image differencing (Jensen 1986), quantifies defoliation by subtracting reflectance in a $Time_2$ image from the reflectance in a co-registered $Time_1$ image. By relating the spectral difference to defoliation on the ground, different levels of defoliation can be quantified. This method was used to monitor spruce-fir decline (Vogelmann and Rock, 1988) and forest defoliation by pear thrips (Vogelmann and Rock, 1989), gypsy moth (Muchoney and Haack, 1994; Nelson, 1983), and HWA in our pilot study (Royle and Lathrop, 1997).

The use of spectral vegetation indices in combination with image differencing to monitor changes in vegetation biomass or leaf area shows great promise. Healthy green vegetation reflects near infrared (NIR) energy and absorbs visible red and middle infrared (MIR) wavelengths of energy. The ratio of NIR/red is positively correlated with the amount of green vegetation present and serves as a useful vegetation index in forest-related studies (Spanner et al., 1990). Numerous vegetation indices have been used in forest defoliation studies, but the best VIs for quantifying changes in green biomass have been the ratio-based indices (e.g., SR and NDVI). The Vegetation Index Difference (VID) method quantifies the increase or decrease in a vegetation index from $Time_1$ to $Time_2$. The VID method has been useful in detecting defoliation because it relates directly to the green biomass present (Nelson, 1983). By comparing Landsat TM images before and after HWA infestation, our 1997 study showed a strong relationship between hemlock defoliation and the VID, based on the Simple Ratio vegetation index. This VID approach has been found useful in other insect defoliations where a general loss of foliage was not necessarily accompanied by a pronounced spectral change (Muchoney and Haack, 1994; Nelson, 1983; Vogelmann and Rock, 1989).

Research goals: The goal of this study was to improve the methodology employed in our pilot study (Royle and Lathrop, 1997) to address the challenges posed by remotely sensed monitoring of forest health discussed above. A more specific objective was to detect and map up to five levels of defoliation in eastern hemlock-mixed hardwoods forest across the heterogeneous landscape of northern New Jersey with high accuracy. An underlying premise of our methodology is that it effectively quantifies differences in canopy and site from $Time_1$ to $Time_2$, while incorporating variation among hemlock sites within a Landsat image with the end result of improving estimates of hemlock forest defoliation.

Materials and Methods

Study area: This study was conducted in the Highlands physiographic province of northern New Jersey, whose topography is characterized by rugged, rolling hills and broad, discontinuous, parallel mountain ridges oriented southwest to northeast. Elevations range from 460 m on the ridge tops to 105 m in the valleys. Slopes vary from gentle (less than 5%) to very steep (greater than 60%). The mature vegetation of this temperate forest community consists of the Mixed Oak forest type of deciduous, broad-leaved species interspersed with stands of the Hemlock-Mixed Hardwoods forest type (Robichaud and Buell, 1973).

Landsat data and processing: We summarize the methodology for processing the imagery for analysis; additional details may be found in Royle (2002). Leaf-off, winter scenes of Landsat TM Imagery of the study area (Path 14, Row 31, 50% downshift) were acquired for 8 November 1984 and 22 December 1994. As hemlock forest is found in hilly to mountainous regions, relief displacement can be a significant source of error (Royle and Lathrop, 1997). To help reduce these positional inaccuracies caused by changes in terrain elevation across the scene (Lillesand and Kiefer, 1994), we used terrain-corrected imagery. It was purchased from the United States Geological Survey EROS Data Center, and rectified to Universal Transverse Mercator projection, North American Datum 1983 with a rectification error of less than 1 pixel (30m).

The 1984 image became the base scene for image-processing and change-detection. Not only was it the pre-infestation data against which all vegetation changes would be compared, it also had the clearest atmospheric conditions. To correct for any atmospheric haze present within each scene, we used the Dark Object Subtraction method, assuming 1% reflectance present in the darkest objects (Chavez, 1988, 1989; Teillet and Fedosejevs, 1995). The darkest objects consisted of deep, clear lakes located in relatively undeveloped, forested areas. Corrections were made to bands 1 through 4, but not bands 5 and 7, because the mid-infrared bands were largely unaffected by atmospheric conditions in the imagery. The corrected digital counts (DN) were converted to radiance using published coefficients (Markham and Barker, 1986).

Our initial work showed that rugged terrain could significantly affect the radiance readings from hemlock stands by depressing radiance on north-facing slopes and enhancing radiance on south-facing slopes, a common effect observed in mountainous areas. We investigated different techniques (topographic normalization) designed to correct these effects (Civco, 1989; Colby, 1991; Smith et al., 1980). However, we found the results to vary widely, so we incorporated a site illumination variable (Shaded Relief; ERDAS Imagine 8.5) in our analyses, instead. Shaded Relief quantifies site illumination for a site and varies from 0 to 1. It is calculated from the slope and aspect per pixel and derived from a digital elevation model (DEM) as well as the solar elevation and solar azimuth for the image date. We used solar data from the 1984 imagery because all scenes were normalized to that scene.

The radiance values were converted to at-canopy reflectance using published formulae (Markham and Barker, 1986). To further remove any remaining temporal differences in solar brightness and other factors, the 1994 scene was normalized to the 1984 base scene using a sample of 200 pseudo-invariant features (water, bare soil, sand, and paved surfaces) and the linear band-wise regression method (Heo and FitzHugh, 2000).

Vegetation indices: Four indices (Table 1) have been found useful in hemlock research (Bonneau et al., 1999; Morton and Young, 2000; Royle and Lathrop, 1997): the Simple Ratio (SR), the Normalized Difference Vegetation Index (NDVI), the Atmospherically Resistant Vegetation Index (ARVI), and the Modified Soil Adjusted Vegetation Index ($MSAVI_2$). The NDVI and SR are derived from the near infrared (NIR, 0.76 to 0.90 μm) and visible red (0.63 to 0.69 μm) wavebands and are functionally similar (Birth and McVey, 1968; Rouse et al., 1973). Weaknesses include sensitivity to atmospheric haze and soil "noise" (Teillet et al., 1997) and saturation at high canopy cover (McDonald et al., 1998). The ARVI is similar to NDVI but reduces atmospheric effects by subtracting the visible blue band (0.45 to 0.52 μm) from the visible red band before the NDVI component is calculated (Huete and Liu, 1994; Kaufman and Tanre, 1992). The $MSAVI_2$ is derived also from NIR and red wavebands, but it employs a correction factor to reduce sensitivity to soil variation across a scene (Qi et al., 1994). The four vegetation indices were calculated for each pixel in the image. The Vegetation Index Difference (VID) was calculated per pixel by subtracting each 1994 vegetation index from the corresponding 1984 vegetation index per pixel. Positive VID values represented defoliation; negative VID values represented growth. Image differencing was performed on the TM bands (1984 to 1994) for bands 1 to 5, and 7 (TMID), because we evaluated these variables as part of our analysis. To reduce potential effects of minor misregistration (Royle and Lathrop, 1997; Townshend et al., 1992), we smoothed all TM and VI data using an algorithm to calculate a 3 × 3 neighborhood mean for each pixel in the image.

TABLE 1. The four multispectral vegetation indices selected for analysis.

Vegetation index	Formula
SR Simple Ratio	SR = NIR/Red Where: NIR is Landsat TM band 4, near infrared wavelengths Red is Landsat TM band 3, visible red wavelengths
NDVI Normalized Difference Vegetation Index	NDVI = (NIR − Red)/(NIR + Red)
$MSAVI_2$ Second Modified Soil Adjusted Vegetation Index	$MSAVI_2 = (2NIR + 1 - ((2NIR + 1)^2 - 8(NIR - Red))^{-1/2})/2$
ARVI Atmospherically Resistant vegetation Index	ARVI = (NIR − RB)/(NIR + RB), Where: RB = Red − γ (Blue − Red) Blue is Landsat TM band 1, visible blue wavelengths γ = 1, unless the aerosol model is known *a priori*

Field data: In the spring and early summer of 1995, we evaluated hemlock canopy condition for 142, circular (90-m-diam.) field plots scattered across the study area and representing a broad range of site characteristics (slope, elevation, and aspect). This plot size was selected to correspond to a 3 × 3 pixel window in a Landsat image. Differentially corrected coordinates obtained with a hand-held Global Positioning System (GPS) unit were used to establish the geographic coordinates for the center of each field plot. Although hemlock defoliation is spatially heterogeneous within stands, discrete levels of defoliation can be recognized in the field. We defined five levels of defoliation on individual trees: Healthy (0%), Light (<25%), Moderate (25% to 50%), Severe (50% to 75%), and Dead (>75%). We surveyed the tree canopy throughout the field plot to develop a

plot-level estimate of defoliation weighted by the amount of hemlock canopy cover per defoliation class (Royle and Lathrop, 1997). Based on the plot-wide estimate of defoliation and our field notes, we assigned each plot to the class that best described the level of defoliation per field plot.

Data and variables for analysis: The sample units for analysis consisted of the 142 field plots. The discrete defoliation class observed in each field plot was the dependent variable. Twenty-one independent, continuous variables were selected for analysis: the four vegetation indices for 1984; the difference in each of the four vegetation indices from 1984 to 1994 (the VIDS); the 1984 reflectance for each of six Landsat TM bands (1–5 and 7); the difference in reflectance for the six Landsat TM bands from 1984 to 1994 (the TMIDs); and Shaded Relief. Using the center coordinates of each field plot, we obtained the values of each variable per field plot from the imagery.

Discriminant function analysis: We used canonical analysis of discriminance (CAD) to discriminate five levels of defoliation. We tested for violations of the assumptions (McGarigal et al., 2000) and found that they were not violated, the linear function was sufficiently robust, and transformations were unnecessary. To evaluate the discriminant function, we examined the squared canonical correlation (R_c^2) and classification accuracy. To assess accuracy, we selected a cross-validation method in which one observation is withheld from the modeling; the model is then applied to the single observation, and the predicted class is compared with the observed class; this is repeated with each observation, and the results are tallied in a classification error matrix (Lachenbruch and Mickey, 1968). We tested this method against other cross-validation methods and concluded that bias, if any, in this method is minimal.

From the resulting cross-validation error matrix, we performed three tests of classification accuracy. The first test was the overall classification accuracy for the five defoliation classes (H, L, M, S, D). Because it is difficult to distinguish lightly defoliated hemlock from healthy hemlock (Morton and Young, 2000; Royle and Lathrop, 1997), we calculated accuracy for a four-class model (HL, M, S, D) as a second test of accuracy. The third test was the accuracy for the three worst defoliation classes (M, S, D), because the cost of misclassification would be higher for these classes in planned future analyses. In addition, we tested for significant differences among the means of the five defoliation classes (F test) and between the means of adjacent defoliation classes (Hotelling T^2).

CAD with TM and VI data: To determine which vegetation index best discriminated hemlock defoliation, we performed CAD on each VID alone. In addition, we performed CAD on each VID together with its 1984 vegetation index (VI) to determine if initial VI values improved the discriminant function. The VI that performed best overall (i.e., had the highest canonical correlation and the highest overall classification accuracy) was selected for further analysis.

An underlying premise of this study was that explaining variation inherent in hemlock sites across the heterogeneous study area would improve accuracy. We attempted to do so using additional Landsat TM bands because different bands are sensitive to water, soil, and vegetation. To avoid singularity, we excluded TM bands from which the best vegetation index was derived (NIR and red). We used stepwise discriminant analysis to select a smaller subset of variables for analysis with the best vegetation index. The CAD was conducted on this subset, systematically adding variables in the order selected by stepwise discriminant analysis. It was also conducted on various combinations of the variables in the subset. We examined the R_c^2 and the three tests of accuracy of each discriminant function and selected the "best" model (i.e., the discriminant function that was parsimonious, ecologically meaningful, and achieved high classification accuracy).

Map of 1994 hemlock defoliation: The linear coefficients from the best discriminant function were applied to the image data to produce a GIS map depicting different levels of defoliation across the study area. We used GIS maps of known hemlock forest stands (Coutros, 1989) to retain only Highlands hemlock stands in the final, thematic map of hemlock defoliation classes. Note that the base map used in this study differs from that used in our 1997 pilot study. The total area per defoliation class was quantified from the resulting GIS data.

Results

Canonical analysis of discriminance: Table 2 summarizes the canonical correlation and classification accuracy of the four vegetation indices and the variables that discriminated five levels of defoliation with the highest classification accuracy. In general, there was a positive, linear relationship between the VID (i.e., the difference in the vegetation index from 1984 to 1994) and the defoliation class for each of the vegetation indices ($P < 0.0001$), indicating that as hemlock defoliation increased, so did the spectral VID (Fig. 1). However, the vegetation indices differed in their ability to discriminate between adjacent classes of defoliation. The VIDs for SR, NDVI, and ARVI, for example, could not discriminate between Healthy and Light defoliation. All three adjacent classes of defoliation from Light to Dead were discriminated only by the VIDs for NDVI and ARVI ($P < 0.05$). Of the four VIDS, NDVI was the best at discriminating defoliation or hemlock condition, as indicated by the R_c^2, and the three tests of classification accuracy (Table 2). The NDVI VID alone explained 64% of the total variation in the canonical function explained by differences in group means, fol-

TABLE 2. Canonical correlation and classification accuracy of the independent variables that discriminated hemlock defoliation with the highest accuracy.

Variables	R_c^2	% Accuracy		
		5-class H, L, M, S, D[1]	4-class HL, M, S, D	MSD
Vegetation Index Difference[2] (VID), ranked by R_c^2				
NDVI	0.64***	34	61	54
ARVI	0.51***	28	53	48
$MSAVI_2$	0.40***	38	46	35
SR	0.33***	36	49	37
Each VID with its 1984 VI, ranked by R_c^2				
SR	0.68***	52	62	54
NDVI	0.68***	51	62	50
$MSAVI_2$	0.60***	44	52	43
ARVI	0.58***	51	62	48
Other variables, ranked by R_c^2				
TMID[3] 1	0.38***	34	48	26
TM 1 for 1984	0.30***	34	44	35
TMID 7	0.30***	25	38	18
Shaded Relief[4]	0.28***	31	39	35
TMID 2	0.26***	30	46	24
TMID 5	0.26***	33	42	26
NDVI for 1984	0.16***	30	29	36
Discriminant function[5]	0.81***	73	82	78

[1] The five health classes are Healthy (H), Light (L), Moderate (M), Severe (S), and Dead (D).
[2] The Vegetation Index Difference (VID) is the difference in the Vegetation Index (either SR, NDVI, ARVI, or $MSAVI_2$) from 1984 to 1994.
[3] TMID is the TM Image Difference, the difference in reflectance from 1984 to 1994 for the respective Landsat TM band.
[4] Shaded Relief quantifies solar illumination based on landform, solar elevation, and solar azimuth of the image date.
[5] The variables in the discriminant function are: the VID for NDVI, the 1984 NDVI, the TMID for Landsat band 1, the 1984 Landsat TM band 1, the TMID for Landsat TM band 2, the TMID for Landsat TM band 5, and Shaded Relief.
*** $p < 0.0001$.
R_c^2 is the canonical R-squared.

lowed by the VIDs for ARVI ($R_c^2 = 0.51$), $MSAVI_2$ ($R_c^2 = 0.40$), and SR ($R_c^2 = 0.33$). The NDVI VID discriminated and classified five classes of hemlock defoliation with 34% accuracy, four classes with 61% accuracy, and the three worst defoliation classes (MSD) with 54% accuracy. Although less accurate in discriminating between Healthy and Light classes, NDVI performed better than the other indices in detecting and classifying unhealthy hemlocks. The performance of the other VIDs varied before and after Healthy and Light were aggregated to calculate the four-class accuracy. Note that canonical correlation was not always indicative of better classification accuracy.

All the 1984 VIs (not shown) were weakly correlated with defoliation ($r < 0.33$), and the ability to discriminate between adjacent classes was low. The 1984 SR and NDVI, for example, could discriminate only between Healthy and Light and between Severe and Dead ($P < 0.05$). However, the 1984 VI together with its corresponding VID increased classification accuracy for each of the VIs (Table 2). The SR performed slightly better than NDVI in the tests of accuracy. For multiple CAD, we report the R_c^2 of the first canonical function. The VID for NDVI and for SR, along with their respective 1984 VI, performed best ($R_c^2 = 0.68$). The ARVI classified levels of defoliation slightly better than $MSAVI_2$.

Adding additional Landsat TM bands to the analysis further increased the ability of the discriminant function to discriminate five levels of defoliation. The box plots for the independent variables reveal that some were nonlinear (Fig. 1). Although each was able to discriminate between certain adjacent classes, only one could discriminate all adjacent classes: TMID 1, the difference in the spectral reflectance from 1984 to 1994 for band 1, visible blue. The TM image difference variable (TMID) most highly correlated with defoliation was TMID 1, followed by 1984 TM 1 (Table 2). The variables other than vegetation indices selected by stepwise DA included (ranked by partial correlation, R_p^2): TMID 1 (visible blue, $R_p^2 = 0.38$), Shaded Relief (site illumination, $R_p^2 = 0.38$), TMID 2 (visible green, $R_p^2 = 0.32$), TMID 5 (mid-infrared, $R_p^2 = 0.19$), and 1984 TM 1 (visible blue, $R_p^2 = 0.14$). These five variables, in addition to the NDVI VID and the 1984 NDVI, were the subset of variables that discriminated defoliation with the highest accuracy (Table 2).

Although the image difference variables were partly derived from the 1984 variables, the correlation matrix shows that NDVI VID and TMID 1 were weakly correlated with their respective 1984 variables, confirming that the inclusion of the 1984 variables was neither singular nor redundant (Table 3). Overall, we did not find multi-collinearity to be a problem, though some redundancy may have been present among the independent variables. Although more parsimonious models (four to five variables) yielded satisfactory levels of accuracy

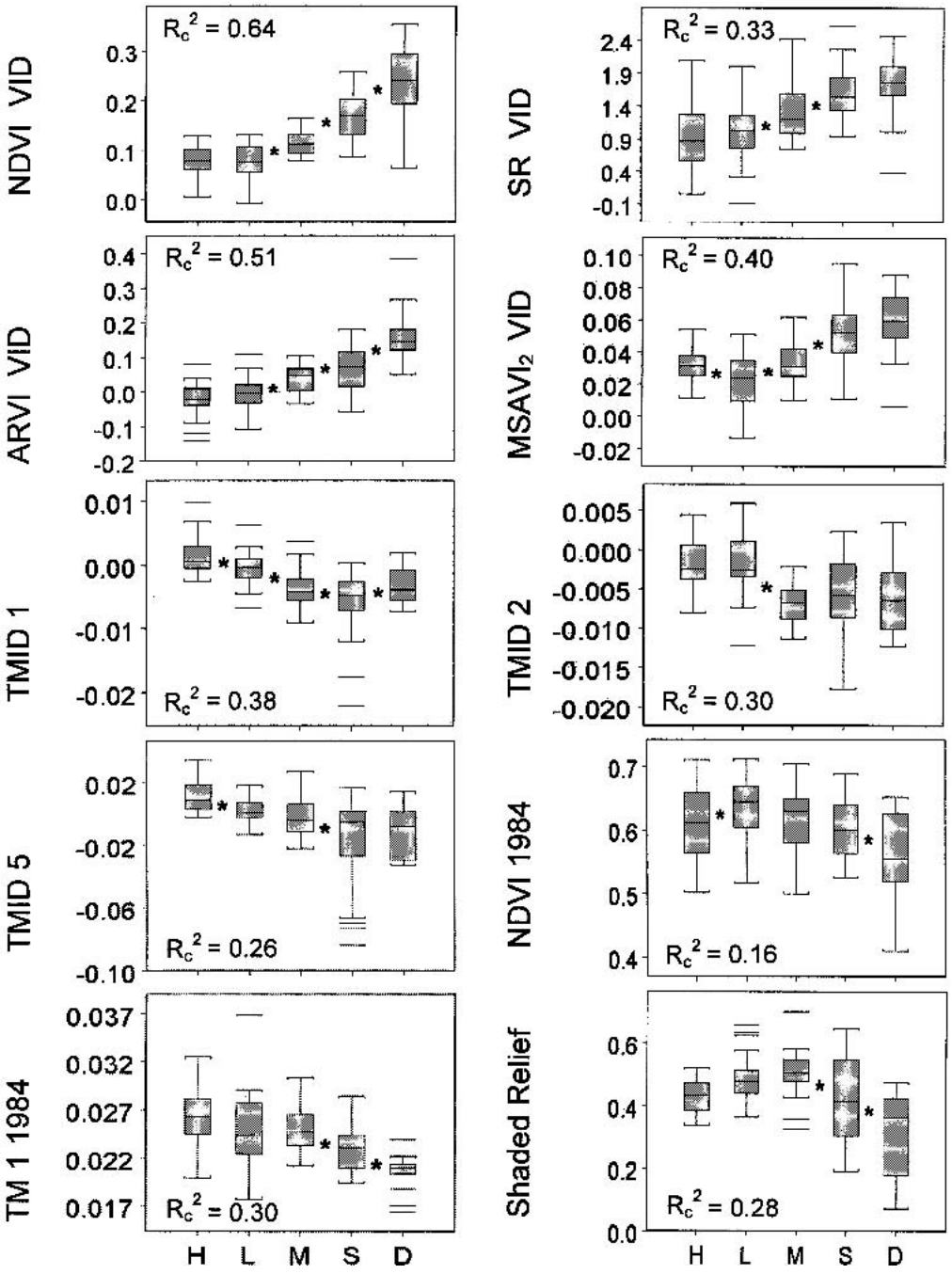

FIG. 1. Box plots of the four VIDs and independent variables per defoliation class. Adjacent classes discriminated by the discriminant function ($P < 0.05$) are marked with an asterisk (*). The defoliation classes are Healthy (H), Light (L), Moderate (M), Severe (S), and Dead (D).

(i.e., 70% or better for four classes and 60% or better for MSD), the best discriminant function with seven variables was 6% to 7% better for four classes, and 13% to 15% better for the MSD classes than discriminant functions with four to five variables.

The canonical structure for the best discriminant function indicates that the first two canonical functions explained 97.5% of the variation in defoliation classes. The first canonical function ($P < .0001$) was most highly correlated with NDVI VID ($r = 0.89$), and the second function ($P < .01$) was most highly correlated with Shaded Relief ($r = -0.64$). Accuracy for the best model was 73% for five classes (H, L, M, S, D) and 82% for four classes (HL, M, S, D), with 78% accuracy for the MSD classes (Table 2). Although all adjacent classes could be discriminated by the best function ($P < 0.01$), there was some confusion between adjacent classes, especially between Healthy and Light (Table 4).

In 1984 there were approximately 6,809 ha of healthy hemlock forest stands across the entire Highlands Prov-

TABLE 3. The correlation matrix for the variables used in the discriminant function that discriminated hemlock health with the highest classification accuracy.

Variables in the CAD function	NDVI VID[1]	NDVI for 1984	TMID Band 1	TM 1 for 1984	TMID Band 2	TMID Band 5	Shaded Relief
NDVI VID	1.00	—	—	—	—	—	—
NDVI for 1984	–0.22	1.00	—	—	—	—	—
TMID Band 1	–0.31	–0.04	1.00	—	—	—	—
TM 1 for 1984	–0.58	–0.04	0.15	1.00	—	—	—
TMID Band 2	–0.19	–0.17	0.54	–0.02	1.00	—	—
TMID Band 5	–0.32	–0.28	0.67	0.22	0.59	1.00	—
Shaded Relief	–0.54	0.45	–0.22	0.63	–0.39	–0.31	1.00

''Band'' refers to a Landsat Thematic Mapper (TM) spectral band. Band 1 represents visible blue wavelengths, Band 2 represents visible green wavelengths, and Band 5 represents mid-infrared wavelengths.

NDVI VID is the Vegetation Index Difference for the NDVI vegetation index, or the difference in NDVI from 1984 to 1994.

TMID is the Thematic Mapper Image Difference, or the difference in reflectance from 1984 to 1994 for a given Landsat band.

Shaded Relief quantifies solar illumination based on landform and the solar elevation and the solar azimuth of the 1984 Landsat image date used as the base scene for analysis.

ince of northern New Jersey. Ten years later nearly half the hemlock forest stands (i.e., pixels) were defoliated to some degree by HWA, with 52% remaining in a Healthy-Light condition, followed by 26% in the Moderate, 16% in the Severe, and 6% in the Dead classes.

DISCUSSION

The success of the VID method relates to three issues involved in accurately classifying hemlock defoliation across a heterogeneous landscape. First, because hemlock canopy cover varies among natural stands, a severely defoliated, dense hemlock stand in 1994 can spectrally resemble an initially sparse, but healthy, hemlock stand elsewhere in the same image. This makes single-scene image classification methods less effective for monitoring hemlock forest health in mixed forests. Although image differencing is promising, there are additional difficulties to consider. The VID alone without the initial VI is not as effective as the two are together in classifying hemlock forest health. For example, it is possible for two hemlock stands bearing the same VID value to represent different defoliation classes; an initially high-cover, 1984 stand that is moderately defoliated by 1994 may have lost the same green biomass as a low-cover, 1984 stand that is dead by 1994. Thus, it is not solely the amount of green biomass lost by any individual stand by $Time_2$ that determines a stand's decline status but rather the loss of biomass relative to its initial starting point.

TABLE 4. The classification matrix of the best discriminant function.

Observed defoliation (rows)	Predicted defoliation (columns)					
	Healthy	Light	Moderate	Severe	Dead	Total
Healthy	<u>16</u>	10	2	0	0	28
Light	4	<u>23</u>	5	0	0	32
Moderate	0	0	<u>21</u>	3	1	25
Severe	0	1	7	<u>24</u>	5	37
Dead	0	0	0	1	<u>19</u>	20
Total	20	34	35	28	25	142

Observed Defoliation is the level of defoliation observed in the field.

Predicted Defoliation is the defoliation class to which a plot was assigned by the discriminant function.

The diagonals (underlined) indicate complete agreement between the observed and predicted classes.

Overall classification accuracy is calculated as the sum of the diagonals divided by the total number of observations.

For NDVI, the inclusion of the 1984 VI value incrementally improved discrimination above and beyond that of the VID alone. The inclusion of the initial VI helps to normalize for heterogeneity across a range of initial stand conditions from largely mixed to almost pure hemlock stands. In this way we avoid the trap of confusing effects (e.g., foliage loss) from determining factors (e.g., stand density) in mapping insect defoliation (Radeloff et al., 1999).

In addition to the VI and VID values, the TMID for the visible blue, visible green, and middle infrared wavebands stood out, though we are not certain of the underlying biophysical reasons for the inclusion of these bands. One possibility is that they help explain for unaccounted differences in atmospheric conditions and background understory vegetation and leaf litter. Another is that these variables together represent a broader range of wavebands (bands 1 through 5) that detect levels of defoliation better than NDVI alone (bands 3 and 4). Bands 3, 4, and 5 are the most useful bands for detecting coniferous forest (Nelson et al., 1984). Band 1 (visible blue) may explain additional atmospheric ''noise'' to which NDVI is sensitive. Band 2 (visible green) may explain additional variation in the canopy missed by the NDVI. Band 5 (MIR) has been found useful in other studies involving forest canopies because mid-infrared wavelengths are sensitive to moisture content in vegetation. Shaded Relief explains variation in site illumination and serves as a substitute for topographic normalization methods, which we found to be problematic.

We may have reached the limit on the classification accuracy that can be attained using the data and methods employed in this study. Distinguishing non-hemlock evergreens in the understory and canopy, for example, is virtually impossible without ancillary data beyond that provided in Landsat imagery.

Discriminant analysis provided a straightforward method of relating the categorical field estimates of hemlock health to spectral reflectance with discriminant functions that could then be applied to predict the hemlock decline status across the entire study area with reasonable accuracy. Based on the three tests of accuracy, NDVI performed best overall, but the results differed among the other vegetation indices when Healthy and Light classes were aggregated. These results were somewhat unexpected in that we assumed

that either ARVI or $MSAVI_2$ would further reduce extraneous factors, resulting in a better model fit. The ARVI is designed to reduce atmospheric influences, and the use of atmospherically corrected imagery may have reduced the effectiveness of ARVI. The $MSAVI_2$ is designed to be less sensitive to differences in background soils in an agricultural setting. As we were working with forests that did not have exposed soils present, though they did have leaf litter in the background, the $MSAVI_2$ may not have been as effective in the VID method.

We have made a number of improvements to increase the accuracy and reliability of the VID change detection technique employing Landsat TM time series imagery to map hemlock defoliation and mortality at the landscape scale. The improvements outlined in this study have increased the accuracy of mapping four classes of defoliation (HL, M, S, D) from 64% in our initial study (Royle and Lathrop, 1997) to 82% in this study. We believe the strength of this study to be the successful incorporation of stand and site heterogeneity across a complex landscape and the effective statistical explanation of that heterogeneity using multivariate analyses and a full complement of appropriate, spectral data.

This study shows that nearly half the hemlock forest stands of the New Jersey Highlands were affected by HWA by 1994. Based on the success of this methodology, we are now using a time series of vegetation index images to investigate temporal and spatial patterns (Royle and Lathrop, 2002) in the infestation and decline process over the past decade and are expanding our study to the entire Mid-Atlantic region of the United States. With additional field reference data collected during autumn 2001, we will test the applicability of this model under different landscape conditions and different time periods. The remotely sensed hemlock decline maps we produce will help produce site-specific management decisions associated with integrated pest management efforts to counteract the spread of HWA as well as plan the silvicultural operations needed to deal with the consequences of hemlock decline and death.

Literature Cited

Bannari, A., D. F. Morin, F. Bonn, and A. R. Huete. 1995. A review of vegetation indices. Remote Sensing Reviews 13:95–120.

Birth, G. G., and G. McVey. 1968. Measuring the color of growing turf with a reflectance spectrophotometer. Agronomy Journal 60: 640–643.

Bonneau, L. R., K. S. Shields, and D. L. Civco. 1999. Using satellite images to classify and analyze the health of hemlock forests infested by the hemlock woolly adelgid. Biological Invasions 1:255–267.

Buchheim, M. P., A. L. MacClean, and T. M. Lillesand. 1985. Forest cover type mapping and spruce budworm defoliation using simulated SPOT imagery. Photogrammetric Engineering and Remote Sensing 51:1115–1122.

Chavez, P. S., Jr. 1988. An improved dark-object subtraction technique for atmospheric scattering correction of multispectral data. Remote Sensing of Environment 24:459–479.

Chavez, P. S., Jr. 1989. Radiometric calibration of Landsat Thematic Mapper multispectral images. Photogrammetric Engineering and Remote Sensing 55:1285–1294.

Cheah, C. A., and M. S. McClure. 2002. *Pseudoscymnus tsugae* in Connecticut forests: The first five years. *In:* J. Lashomb, B. Onken, K. Shields, J. Linnane, D. Souto, R. Rhea, and R. Reardon, eds. Proceedings of the Hemlock Woolly Adelgid Symposium. East Brunswick, NJ, 5–7 February 2002. USDA Forest Service Technical Report, in press.

Civco, D. L. 1989. Topographic normalization of Landsat Thematic Mapper digital imagery. Photogrammetric Engineering and Remote Sensing 55(9):1303–1309.

Colby, J. D. 1991. Topographic normalization in rugged terrain. Photogrammetric Engineering and Remote Sensing 57(5):531–537.

Coppin, P. R., and M. E. Bauer. 1996. Digital change detection in forest ecosystems with remote sensing imagery. Remote Sensing Reviews 13:207–234.

Coutros, C. 1989. GIS map: Eastern Hemlock of New Jersey. New Jersey Department of Environmental Protection, Trenton, NJ.

Evans, R. A., E. Johnson, J. Shreiner, A. Ambler, J. Battles, N. Cleavitt, T. Fahey, J. Sciascia, and E. Pehek. 1996. Potential impacts of hemlock woolly adelgid (*Adelges tsugae*) on eastern hemlock (*Tsuga canadensis*) ecosystems. Pp. 42–57 *in* S. M. Salom, T. C. Tigner, and R. C. Reardon, eds. Proceedings of the First Hemlock Woolly Adelgid Review; 12 October 1995; Charlottesville, VA. USDA Forest Service FHTET 96-10.

Franklin, S. E. 1989. Classification of hemlock looper defoliation using SPOT HRV imagery. Canadian Journal of Remote Sensing 15: 178–182.

Franklin, S. E., and A. G. Raske. 1994. Satellite remote sensing of spruce budworm forest defoliation in western Newfoundland. Canadian Journal of Remote Sensing 20:37–48.

Heo, J., and T. W. FitzHugh. 2000. A standardized radiometric normalization method for change detection using remotely sensed imagery. Photogrammetric Engineering and Remote Sensing 66:173–181.

Huete, A. F., and H. Q. Liu. 1994. An error and sensitivity analysis of the atmospheric- and soil-correcting variants of the Normalized Difference Vegetation Index for the MODIS-EOS. IEEE Transactions in Geoscience and Remote Sensing 32:897–905.

Jensen, J. R. 1986. Introductory digital image processing. Upper Saddle River, NJ: Prentice Hall.

Kaufman, Y. J., and D. Tanre. 1992. Atmospherically Resistant Vegetation Index (ARVI) for EOS-MODIS. IEEE Transactions in Geoscience and Remote Sensing 30:261–270.

Lachenbruch, P. A., and M. A. Mickey. 1968. Estimation of error rates in discriminant analysis. Technometrics 10:1–10.

Lachowski, H. P., P. Maus, and B. Platt. 1992. Integrating remote sensing with GIS: Procedures and examples from the Forest Service. Journal of Forestry 12:16–21.

Lashomb, J., B. Onken, K. Shields, J. Linnane, D. Souto, R. Rhea, and R. Reardon, eds. 2002. Proceedings of the Hemlock Woolly Adelgid Symposium. East Brunswick, NJ, 5–7 February 2002. USDA Forest Service Technical Report, in press.

Leckie, D. G., and D. P. Ostaff. 1988. Classification of airborne Multispectral Scanner data for mapping current defoliation caused by the spruce budworm. Forest Science 34:259–275.

Lillesand, T. M., and R. W. Kiefer. 1994. Remote sensing and image interpretation, 3rd ed. New York, NY: John Wiley and Sons.

Markham, B. L., and J. L. Barker. 1986. Landsat MSS and TM post-calibration dynamic ranges, exoatmospheric reflectances, and at-satellite temperatures. EOSAT Landsat Technical Notes 1:3–8.

McClure, M. S. 1987. Biology and control of hemlock woolly adelgid. Bulletin 851, Connecticut Agricultural Experiment Station, New Haven.

McClure, M. S. 1990. Role of wind, birds, deer, and humans in the dispersal of hemlock woolly adelgid (Homoptera: Adelgidae). Environmental Entomology 19:36–43.

McDonald, A. J., F. M. Gemmell, and P. E. Lewis. 1998. Investigation of the utility of spectral vegetation indices for determining in-

formation on coniferous forests. Remote Sensing of Environment 66:250–272.

McGarigal, K., S. Cushman, and S. Stafford. 2000. Multivariate statistics for wildlife and ecology research. New York, NY: Springer-Verlag.

McManus, K. A., K. S. Shields, and D. R. Souto, eds. 1999. Proceedings: Symposium on Sustainable Management of Hemlock Ecosystems in Eastern North America, 22–24 June 1999; Durham, NH. USDA Forest Service GTR NE-267.

Morton, D. D., and J. A. Young. 2000. Relationships of vegetation indices to eastern hemlock (*Tsuga canadensis*) health and stand conditions. *In* Proceedings of the American Society of Photogrammetry and Remote Sensing; 22–26 May 2000; Washington, D.C.

Muchoney, D. M., and B. N. Haack. 1994. Change detection for monitoring forest defoliation. Photogrammetric Engineering and Remote Sensing 60:1243–1251.

Nelson, R. F. 1983. Detecting forest canopy change due to insect activity using Landsat MSS. Photogrammetric Engineering and Remote Sensing 49:1303–1314.

Nelson, R. F., R. S. Latty, and G. Mott. 1984. Classifying northern forests using Thematic Mapper Simulator data. Photogrammetric Engineering and Remote Sensing 50:607–617.

Onken, B. P. 2002. Hemlock woolly adelgid—a race in time. *In* J. Lashomb, B. Onken, K. Shields, J. Linnane, D. Souto, R. Rhea, and R. Reardon, eds. Proceedings of the Hemlock Woolly Adelgid Symposium. East Brunswick, NJ, 5–7 February 2000. USDA Forest Service Technical Report, in press.

Qi, J., A. Chehbouni, A. R. Huete, Y. H. Kerr, and S. Sorooshian. 1994. A modified soil adjusted vegetation index. Remote Sensing of Environment 48:119–126.

Quimby, J. W. 1996. Value and importance of hemlock ecosystems in the eastern United States. Pp. 1–8 *in* S. M. Salom, T. C. Tigner, and R. C. Reardon, eds. Proceedings of the First Hemlock Woolly Adelgid Review; 12 October 1995; Charlottesville, VA. USDA Forest Service. FHTET 96-10.

Radeloff, V. C., D. J. Mladenoff, and M. S. Boyce. 1999. Detecting jack pine budworm defoliation using spectral mixture analysis: Separating effects from determinants. Remote Sensing of Environment 69:156–169.

Robichaud, B., and M. Buell. 1973. Vegetation of New Jersey. New Brunswick, NJ: Rutgers University Press.

Rouse, J. W., R. H. Haas, J. A. Schell, and D. W. Deering. 1973. Monitoring vegetation systems in the Great Plains with ERTS. Proceedings, Third ERTS Symposium 1:48–62.

Royle, D. D. 2002. A landscape analysis of hemlock decline in New Jersey. PhD dissertation, Rutgers University, New Brunswick, NJ, in press.

Royle, D. D., and R. G. Lathrop. 1997. Monitoring hemlock forest health in New Jersey using Landsat TM data and change detection techniques. Forest Science 43:327–335.

Royle, D. D., and R. G. Lathrop. 2002. Using Landsat imagery to quantify temporal and spatial patterns in hemlock decline. *In* J. Lashomb, B. Onken, K. Shields, J. Linnane, D. Souto, R. Rhea, and R. Reardon, eds. Proceedings of the Hemlock Woolly Adelgid Symposium. East Brunswick, NJ, 5–7 February 2002. USDA Forest Service Technical Report, in press.

Salom, S. M., T. C. Tigner, and R. C. Reardon, eds. 1996. Proceedings of the First Hemlock Woolly Adelgid Review; 12 October, 1995; Charlottesville, VA. USDA Forest Service FHTET 96-10.

Singh, A. 1989. Digital change detection techniques using remotely sensed data. International Journal of Remote Sensing 10:989–1003.

Smith, J. A., T. L. Lin, and K. J. Ranson. 1980. The Lambertian assumption and Landsat data. Photogrammetric Engineering and Remote Sensing 46:1183–1189.

Souto, D., T. Luther, and B. Chianese. 1996. Past and current status of HWA in eastern and Carolina hemlock stands. Pp. 9–15 *in* S. M. Salom, T. C. Tigner, and R. C. Reardon, eds. Proceedings of the First Hemlock Woolly Adelgid Review; 12 October 1995; Charlottesville, VA. USDA Forest Service. FHTET 96-10.

Spanner, M. A., L. L. Pierce, D. L. Peterson, and S. W. Running. 1990. Remote sensing of temperate coniferous forest leaf area index: The influence of canopy closure, understory vegetation, and background reflectance. International Journal of Remote Sensing 11:95–111.

Stoetzel, M. B. 2002. History of the introduction of *Adelges tsugae* based on voucher specimens in the SI National Collection of Insects. *In* J. Lashomb, B. Onken, K. Shields, J. Linnane, D. Souto, R. Rhea, and R. Reardon, eds. Proceedings of the Hemlock Woolly Adelgid Symposium. East Brunswick, NJ, 5–7 February 2002. USDA Forest Service Technical Report, in press.

Teillet, P. M., and G. Fedosejevs. 1995. On the dark target approach to atmospheric correction of remotely sensed data. Canadian Journal of Remote Sensing 21:374–387.

Teillet, P. M., K. Staenz, and D. J. Williams. 1997. Effects of spectral, spatial, and radiometric characteristics on remote-sensing vegetation indices of forested regions. Remote Sensing of Environment 61:139–149.

Townshend, J. R. G., C. O. Justice, C. Gurney, and J. McManus. 1992. The impact of misregistration on change detection. IEEE Transactions in Geoscience and Remote Sensing 30:1054–1060.

Vogelmann, J. E., and B. N. Rock. 1988. Assessing forest damage in high-elevation coniferous forests of Vermont and New Hampshire using Landsat Thematic Mapper data. Remote Sensing of Environment 24:227–246.

Vogelmann, J. E., and B. N. Rock. 1989. Use of Thematic Mapper data for the detection of forest damage caused by the pear thrips. Remote Sensing of Environment 30:217–225.

Williams, D., M. E. Montgomery, and K. S. Shields. 2002. *In* J. Lashomb, B. Onken, K. Shields, J. Linnane, D. Souto, R. Rhea, and R. Reardon, eds. Proceedings of the Hemlock Woolly Adelgid Symposium. East Brunswick, NJ, 5–7 February 2002. USDA Forest Service Technical Report, in press.